Rio Oil & Gas Expo and Conference 2020

ISSN 2525-7579

Conference Proceedings homepage: https://biblioteca.ibp.org.br/riooilegas/en/

Technical Paper

Analytical and numerical modeling of through-tubing acoustic logging

Tiago de Magalhães Correia [1]
Luis Paulo Brasil de Souza [2]
Juan Andres Santisteban Hidalgo [3]
Mateus Gheorghe de Castro Ribeiro [4]
Isabel Giron Camerini [5]
Bruno Greco de Sousa [6]
Alan Conci Kubrusly [7]
Helon Vicente Hultmann Ayala [8]
João Humberto Guandalini Batista [9]
Rafael Valladares de Almeida [10].

1. PUC-RIO, ENGENHARIA MECâNICA, . RIO DE JANEIRO - RJ - BRASIL, tiago@puc-rio.br
2. PUC-RIO, ENGENHARIA MECâNICA, . RIO DE JANEIRO - RJ - BRASIL, luisbrasil55@gmail.com
3. PUC-RIO, ENGENHARIA MECâNICA, . RIO DE JANEIRO - RJ - BRASIL, juan_andres@puc-rio.br
4. PUC-RIO, ENGENHARIA MECâNICA, . RIO DE JANEIRO - RJ - BRASIL, mateus-gheorghe@puc-rio.br
5. PUC-RIO, ENGENHARIA MECâNICA, . RIO DE JANEIRO - RJ - BRASIL, isabelc@puc-rio.br
6. OURO NEGRO TECNOLOGIAS, ENGENHARIA, . RIO DE JANEIRO - RJ - BRASIL, bruno.greco@ouronegro.com.br
7. PUC-RIO, CENTRO DE ESTUDOS EM TELECOMUNICAç??ES (CETUC) , . RIO DE JANEIRO - RJ - BRASIL, alan@cpti.cetuc.puc-rio.br
8. PUC-RIO, ENGENHARIA MECâNICA, . RIO DE JANEIRO - RJ - BRASIL, helon@puc-rio.br
9. REPSOL SINOPEC BRASIL, RIO DE JANEIRO, . RIO DE JANEIRO - RJ - BRASIL, joao.batista@repsolsinopec.com
10. REPSOL SINOPEC BRASIL, RIO DE JANEIRO, . RIO DE JANEIRO - RJ - BRASIL, rafael.valladares@repsolsinopec.com

Abstract

Presently, prior to plug & abandonment (P&A) operations, inspection of cement quality executed through acoustic logging techniques requires the removal of the production tubing. Hence, there has been an increasing interest in the industry to provide technological solutions that allow the assessment of cement sealing quality by performing through-tubing logging runs, thus reducing costs associated with P&A operations. This contribution addresses the problem of modeling acoustic wave propagation in multistring wells using both analytical and numerical techniques. Analytical results obtained in the frequency domain for the dispersion spectra of guided waves propagating in the wellbore were employed to validate the numerical simulations via the Finite Element Method (FEM). The effect of different defects in the cement sheath on the dispersion of guided waves in the multistring wellbore and acoustic response to a monopole source were investigated. Results of simulations demonstrated that it is possible to distinguish data from cases with and without the defects.

Keywords: P&A. cement quality. through-tubing logging. guided waves

Received: February 20, 2020 | **Accepted:** Jun 06, 2020 | **Available online:** Dec 01, 2020
Article Code: 099
Cite as: Rio Oil & Gas Expo and Conference, Rio de Janeiro, RJ, Brazil, 2020 (20)
DOI: https://doi.org/10.48072/2525-7579.rog.2020.099

1. Introduction

Encircled by the rock formation, an oil well is composed of several, ideally, cylindrical and concentric layers, namely the production tubing, one or more casing pipes filled with fluids in their annuli, and the cement, which provides structural support while also being responsible for preventing leakage of fluids to the surrounding environment. During its service life, a well experiences significant changes in operational parameters, such as pressure, temperature, and fluid properties, which may damage the cement layer and result in loss of containment (Liu, 2017; Saxena et al., 2018; Østerbo, 2014). At the end of its useful life, the well must be deactivated going through an operation known in the industry as plug and abandonment, or simply P&A (Øia, 2018). Performing an assessment of the cement layer integrity is an essential stage of these operations (Khalifeh & Saasen, 2020).

There are several methods to evaluate the quality of the cement layer prior to P&A, such as hydraulic or differential pressure tests, temperature data, radioactive procedures or through sonic and ultrasonic inspections. Amongst all cement evaluation methods, the most used are those based on sonic and ultrasonic loggings, as they allow effective evaluations of the cement quality and the possibility fluid leakages (Øia, 2018). Cement bond logging tools (CBT) have been employed in the oil and gas industry since the late 1950's (Wang et al., 2016). The first tools relied on cement bond (CBL) and variable density (VDL) sonic log profiles to directly measure cement quality and its bonds to casing and formation (Saxena et al., 2018; Wang et al., 2016). But conventional CBT tools are not able to inspect a well through the tubing, which therefore has to be removed prior to the inspection. This operation significantly increases costs of P&A operations (Øia, 2018; Zhang et al. 2019). Hence, there has been a growing interest in tools capable of performing through-tubing acoustic logs with the tubing still installed in the well (Quintero et al., 2016; Fan et al., 2019). However, the presence of the tubing metallic layer can strongly hinder the analysis and diagnostic of through-tubing well inspection (Viggen et al., 2016a; Viggen et al., 2016b; Talberg et al., 2017). Recent studies have shown that the use of acoustic waves guided in the wellbore may provide effective techniques to analyze the cement condition with the production tubing still in place (Liu et al., 2017; Viggen et al., 2016b).

Looking at this challenging problem, the present contribution reports the use of an analytical-numerical technique to solve the characteristic equations of guided wave propagation in a layered cylinder, which can be used to model a multi-string wellbore. Additionally, defects are introduced in the model in order to simulate how their presence in the cement layer interact with the acoustic, guided waves' dispersion spectra. Numerical simulations via the finite element method (FEM) were also performed and results compared with those of the analytical model in order to assess the accuracy of both approaches. By changing parameters related to different types of defects, it was possible to understand how each of them affect the dispersion spectrum and how the guided modes vary in the presence of defects in the cement sheath.

2. Analytical model

In order to model the propagation of guided waves in a multilayered cylinder we have employed a formulation proposed by Braga et al. (1990) and Braga & Rivas (2005). This approach relies on a recursive algorithm, based on exact solutions for the linear elastodynamics' equations, to obtain and numerically solve the dispersion equation for guided waves propagating in a medium composed of multiple, concentric, uniformly-thick, homogeneous and isotropic cylindrical layers of elastic solids or acoustic fluids. The algorithm was developed as a function of three parameters: the angular frequency, ω, the wavenumber in the axial direction, k_z, and an integer representing the cylindrical harmonics order, ν, being 2ν the number of poles in a cylindrical multipole distribution (e.g., Boerboon et al., 1985).

The algorithm relies on imposing the proper boundary conditions at each interface of the multilayered cylindrical structure that models the wellbore. By employing these continuity condition between successive cylindrical layers, one obtains the global, surface impedance tensor at the top of the last layer G_n (Braga et al., 1990).

Applying this procedure in order to obtain the dispersion spectrum for guided waves in the cylindrical multilayered medium, one fixes ν and search for the pairs of $\omega$and k_z that solves the dispersion equation obtained using the homogeneous boundary condition at the last interface. For an interface between cement and rock formation, two elastic media, the dispersion equation is written as:

$$\det\left[\boldsymbol{G}_n + \boldsymbol{Z}_1^{[n+1]}(r_{n+1})\right] = 0 \quad (1)$$

where $\boldsymbol{Z}_1^{[n+1]}(r_{n+1})$ is the impedance of outgoing waves that propagate or decay through the rock formation.

Equation 1 is solved numerically for pairs ω and k_z that satisfy the outgoing boundary condition at the cement/rock interface. For subsonic waves, ω and k_z are both real numbers and $\omega/k_z < c_S$, where c_S is the speed of the s-wave in the rock formation. After finding the pairs (ω, k_z) that solve the dispersion equation, the solutions are plotted in the form of slowness curves that represent the inverse of the speed of subsonic acoustic wave modes propagating freely through the wellbore.

3. Well configuration and cement defects

Acoustic properties for the layers in the well are listed in Table 1, where ρ is the medium density, λ and μ the Lamé elastic parameters, and c_p and c_s represent, respectively, the p- and s-wave speeds. In the simulations, the tubing and A-annulus are filled with water. The geometrical properties are presented in Table 2.

Table 1 – List of acoustic properties.

Layer	ρ (kg/m^3)	λ (Pa)	μ (Pa)	c_p (m/s)	c_s (m/s)
Steel	7,800	1.10E+11	8.00E+10	5,880	3,200
Water	1,000	2.25E+09	-	1,500	-
Cement	1,800	5.43E+09	5.39E+09	3,000	1,730
Rock (Sandstone)	2,300	1.43E+10	1.62E+10	4,500	2,650

Source: produced by the author

Table 2 – Well configuration parameters, displayed both in inches and meters.

Tubing ID	Tubing OD	Casing ID	Casing OD	Cement Thickness
3.958”	4.500”	8.535”	9.625”	0.5”
0.100 m	0.102 m	0.217 m	0.244 m	0.013 m

Source: produced by the author

A decrease in cement thickness is a defect that deserves attention because it compromises the structure of the well. This defect appears due to corrosion caused by fluids in contact with the cement sheath, being often found in aging oil wells (Østerbo, 2014). As the cement layer becomes thinner, it debonds from the casing or formation. In order to model debonding of the cement sheath with the casing (inner debonding) or the rock formation (outer debonding), a thin fluid layer is inserted between one or the other of the two interfaces (Figure 1). In both cases, inner and outer debonding, the distance from the outer radius of the casing to the inner radius of the rock interface was kept fixed at 0.5” (0.013 m), while the thickness of the debonding layer changed from 0 to 20%, 40% and 60% of the original cement layer thickness (0.5”). The inner and outer debonding are labelled in reference to interface it belongs, i.e., SC stands for Steel/Casing interface and CR for Cement/Rock. Table 3 presents the defects that were analyzed in this paper.

Figure 1 – Schematics of: (a) inner; and (b) outer debonding.

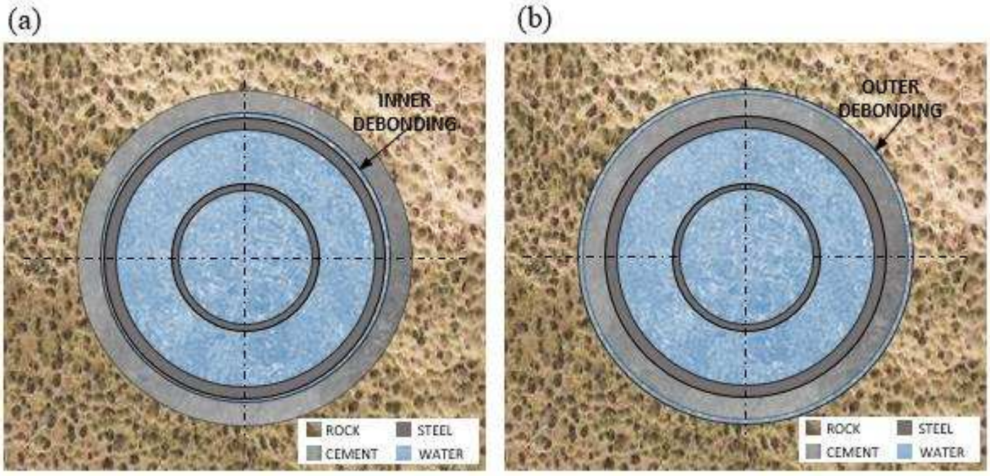

Source: produced by the author

Table 3 – Inner and outer debonding.

Defects	Inner debonding (SC)	Outer debonding (CR)
Severity range	20%, 40%, 60%	20%, 40%, 60%

Source: produced by the author

4. Results

In this section, analytical results for single-casing and through-tubing configurations are obtained from the methods discussed in Section 2. The defect models presented in Section 3 are used to analyze the influence of the defects on the slowness curves.

4.1. Inner Debonding (SC)

Figure 2(a) shows the dispersion spectra in terms of the slowness for the single-casing well with inner debonding of different severities. One readily notices that some of the modes are more sensitive not only to the presence but also to the severity of the defects. The most evident is the one with higher slowness, above that of the bulk acoustic wave in the fluid which corresponds to 666 µs/m. But so are the crossing modes, which are also indicated by arrows in Figure 2(a). The other modes do present variations, however, only due to presence of a defect, being undistinguishable for defects with diverse severities, which are represented here by different thicknesses of the thin fluid layer that fills the debonded interface (see Figure 1).

The dispersion spectra for the well in the through-tubing configuration with a defect at the casing/cement interface are presented in Figure 2(b). As observed for the Single-Casing case, the most significant variations due to the presence of debonding occur in the mode with slowness higher than 666 µs/m as well as in the crossing modes indicated in Figure 2(b). Again, other modes present variation only due to the presence of the defect, being undistinguishable with respect to the defect severity.

Figure 2 – Dispersion spectra obtained by the analytical model for the inner debonding (SC) in the: (a) single-casing configuration; and (b) in the through-tubing configuration. The blue line corresponds to the non-defective case.

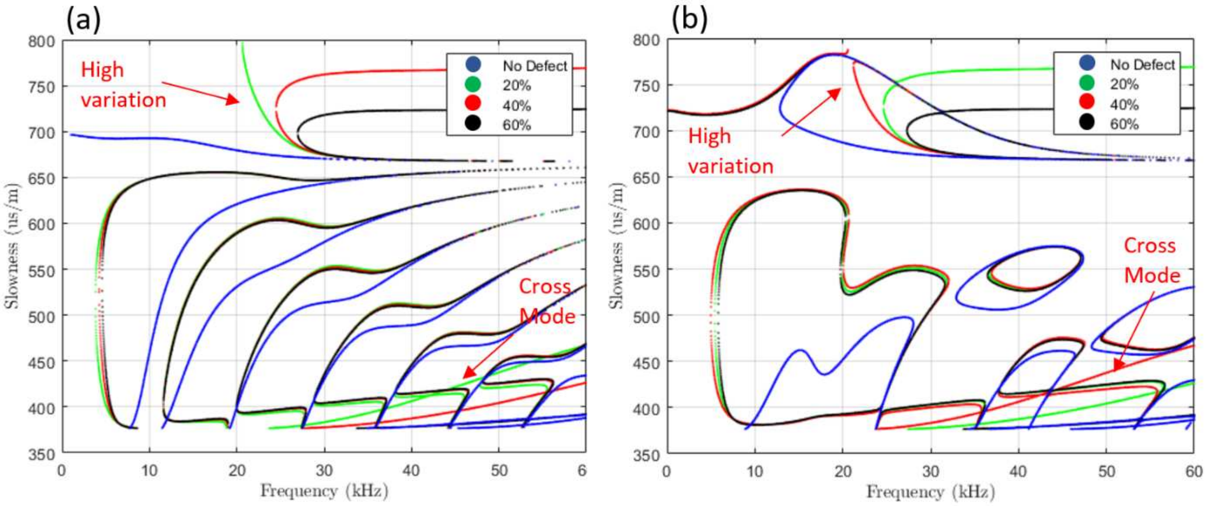

Source: produced by the author

4.2. Outer Debonding (CR)

Figure 3(a) presents the dispersion spectra for the single-casing well with outer debonding. The most significant variations due to the defect occur next to inflection points of the slowness curves. Interestingly, the mode with slowness higher than 666 us/m no longer presents observable changes in in the presence of this defect. The dispersion spectra for the through-tubing well configuration is shown in Figure 3(b). In this case, for defect severities of 40% and 60%, there are closed-loop slowness modes which are not present in the case of a debonding layer with thickness of 20% with respect to the non-defective cement layer.

5. Numerical FEM comparison

Finite element simulations using the commercial software COMSOL Multiphysics© were performed in order to assess the accuracy of both methods. The numerical, axisymmetric model, simulated a monopole acoustic source positioned at the origin of the cylindrical coordinate system. Acoustic pressure fluctuations were recorded at 1,830 equally-spaced positions (probes) along the symmetry axis of the well. The first probe was located at the axial coordinate $z = 152.4$ mm (6") and the last at $z = 1.9812$ m (6½ ft). Choice for this configuration was based on the typical architecture of commercial cement bond logging tools that have an array of receivers used to generate the dispersion curves. Figure 4 depicts the FEM domain for the single-casing configuration. Figure 5 presents the time history of recorded acoustic pressure fluctuations at some of the probes.

Figure 3 – Dispersion spectra obtained by the analytical model for the outer debonding (CR): (a) in the single-casing; and (b) in the through-tubing configuration. The blue line corresponds to the non-defective case.

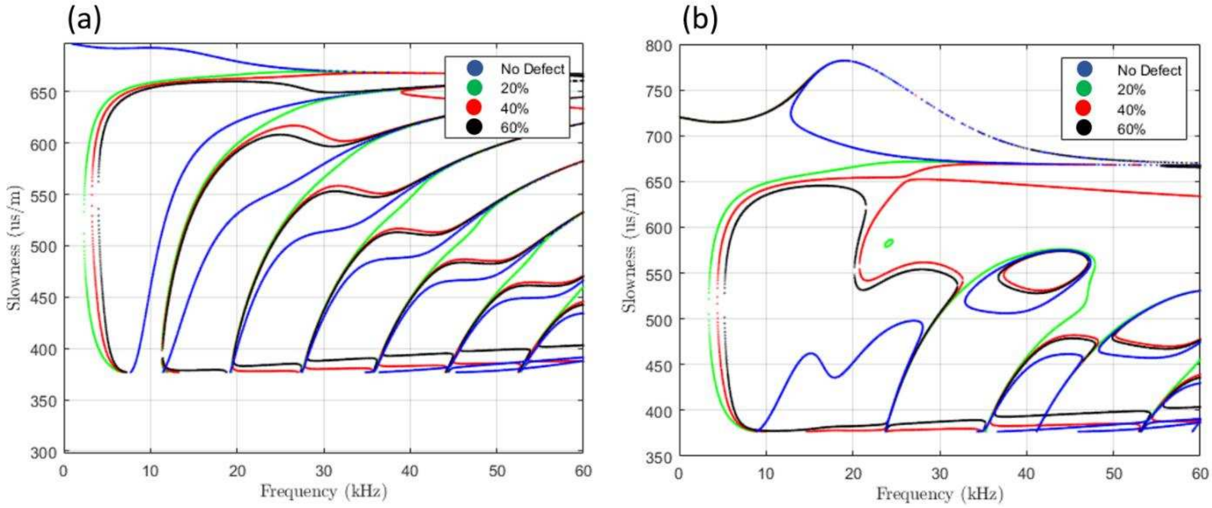

Source: produced by the author

Figure 4 – Axial position of probes. Mech used in COMSOL Multiphysics© simulation.

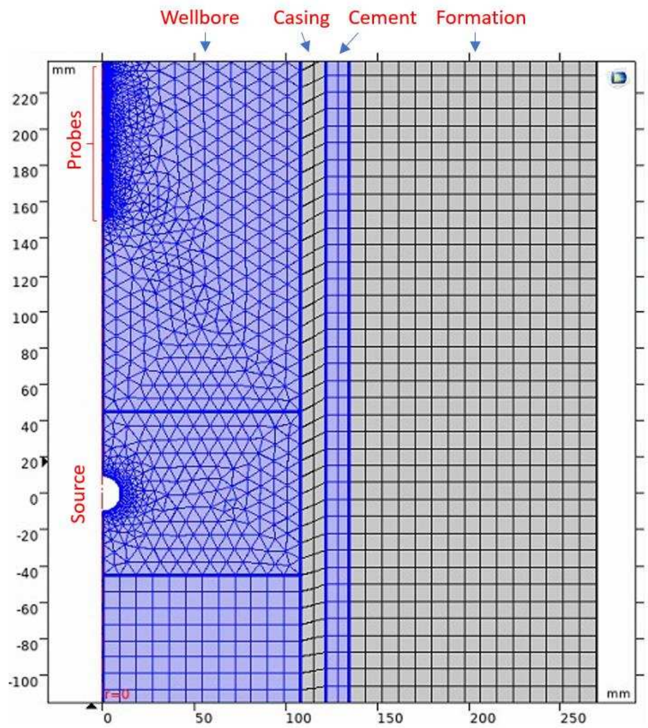

Source: produced by the author

Using a 2D-FFT operation to process the signals recorded by each probe in the time-domain, one obtains the slowness curves of the guided wave modes propagating n the wellbore (Pluta, 2002). Those are shown Figure 6 for the single-casing well configuration with the non-defective cement layer. Black lines in Figure 6 represent the slowness curves obtained by the analytical procedure discussed in Section 4. The agreement between analytical and numerical results is very good. However, the mode with highest slowness is not captured in the FEM model, meaning that its amplitude is small compared to those of other modes and therefore is not captured in the FEM frequency analysis.

Figure 5 – Time-history of acoustic pressure fluctuations at some of the probes.

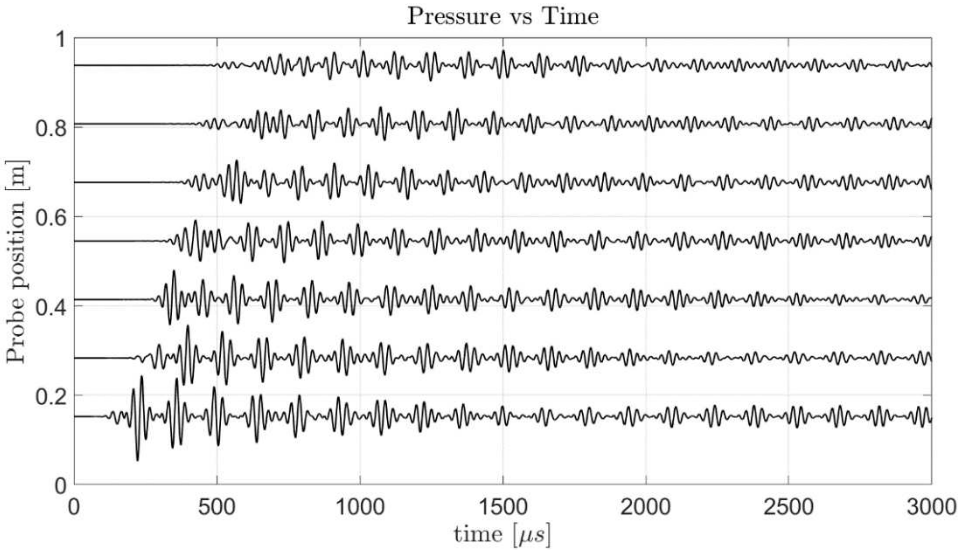

Source: produced by the author

Figure 6 – Slowness curves for the single-casing configuration with non-defective cement.

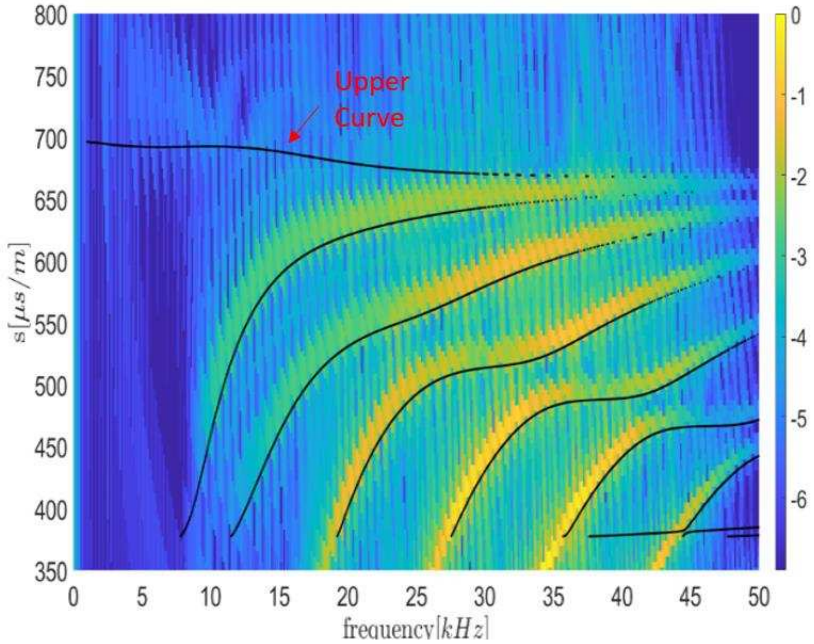

Source: produced by the author

6. Quantitative analysis of mode sensitivity to defects

Figure 7 reproduces the slowness curves previously presented for the single-casing and through-tubing well configurations with non-defective cement. In the plot, color dots indicate the guided wave modes for which the analysis of variations in the slowness due to the presence of defect with different severities was carried out. Tables 4 and 5 presents, for single-casing and though-tubing configurations, respectively, the intensity of slowness variation with the defect, i.e., the measured change in slowness at a fixed frequency when taking that for the non-defective cement as a reference value. Results in Table 4 show that mode R1 is the most promising one for identifying the presence of a defect in the single-casing configuration, exhibiting higher variations in slowness for both inner and outer debonding. However, the slowness at this frequency, close to 10 kHz, changes very little for the R1 mode as the defect, either inner or outer debonding, becomes more severe. Except for mode G3 at close to 30 kHz, this is also the case for all other modes listed in Table 4, meaning that none of these but G3 would be able to efficiently distinguish between defects with different severities.

For the through-tubing configuration, we observe from the results in Table 5 that the interesting modes are G1 and G2. For both inner and outer debonding, these modes are those presenting the highest slowness variation due to the presence of the defect. However, as for all other modes in this case, they are not sensitive to the intensity of the defect, represented by the thickness of the thin fluid layer filling the debonded interface.

Figure 7 – Slowness curves for the (a) single-casing; and (b) through-tubing configuration and non-defective cement. The blue, red, and green dots are the guided wave modes for which the analysis was done.

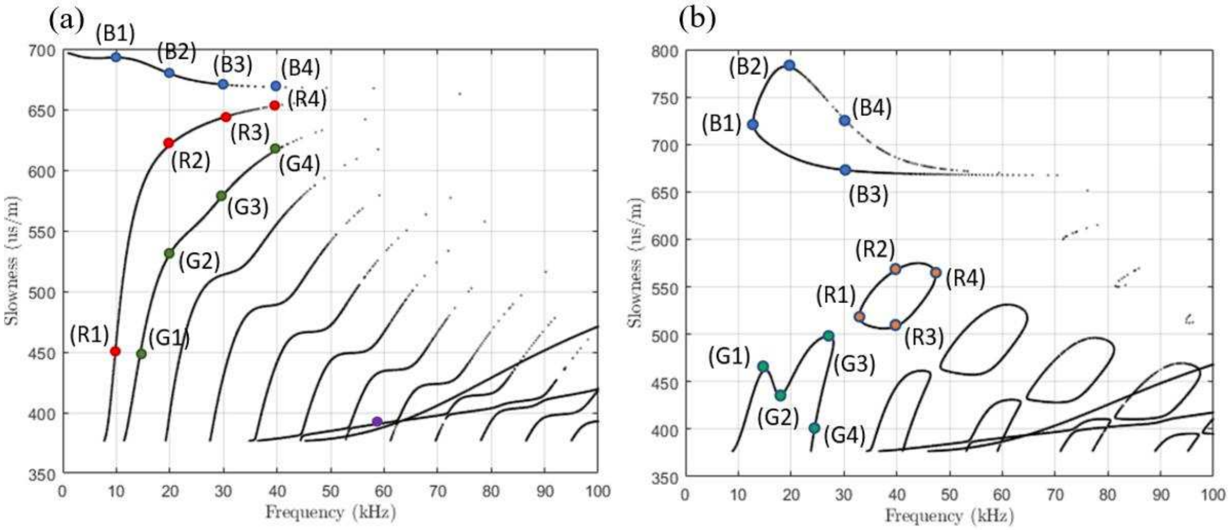

Source: produced by the author

Table 4 – Slowness changes for modes indicated in Figure 4(a) due to the presence of inner and outer debonding of the cement layer in the single-casing well configuration.

Modes	Frequency (kHz)	Slowness for the non-defective cement ($\mu s/m$)	SC Variation ($\mu s/m$) 20%	40%	60%	CR Variation ($\mu s/m$) 20%	40%	60%
B1	10.14	692.7	-	-	-	-	-	-
B2	20.96	678	-	-	-	-	-	-
B3	28.09	671.3	-	-	-	-	91	47
B4	39.37	668.4	-	-	-	-	97	54
R1	9.86	452.6	206	203	201	196	196	196
R2	20.50	622.6	44	40	37	33	33	33
R3	30.90	644.6	26	25	5	3	3	3
R4	40.96	653.7	15	15	0	0	0	0
G1	14.64	452.8	81	81	81	78	78	78
G2	20.72	535.7	64	60	57	55	55	55
G3	30.17	580.4	63	27	17	17	17	17
G4	39.93	616.4	37	0	0	0	0	0

Source: produced by the author

Table 5 – Slowness changes for modes indicated in Figure 4(b) due to the presence of inner and outer debonding of the cement layer in the through-casing well configuration.

Modes	Frequency (kHz)	Slowness for the non-defective cement ($\mu s/m$)	SC Variation ($\mu s/m$) 20%	40%	60%	CR Variation ($\mu s/m$) 20%	40%	60%

B1	12.9	727.4	-	17	17	0	0	0
B2	20.26	780.4	-	0	0	0	0	0
B3	30.64	672.6	7	7	7	0	0	0
B4	30.13	726.5	36	-	6	0	0	0
R1	32.92	518.7	-	-	-	-	-	-
R2	40.78	570.2	0	0	0	0	0	0
R3	39.17	507	19	19	19	49	26	22
R4	47.21	566.1	0	0	0	42	0	0
G1	15.44	461.8	174	174	174	196	189	183
G2	18.43	437.4	192	192	192	225	215	207
G3	24.64	496.8	51	53	55	0	62	55
G4	27.65	406.3	0	0	0	0	0	0

Source: produced by the author

6. Final considerations

This paper investigated how the presence of defects in the cement layer affects the dispersion spectra of acoustic guided waves propagating in a wellbore. In particular, close attention was paid to the through-tubing configuration, which still represents a challenge to employ acoustic logging tools to perform cement evaluations prior to P&A operations. The cases reported here are related to debonding defects, either at the casing/cement or cement/formation interfaces. Both analytical and numerical approaches where employed, the latter via FEM simulation.

Interesting conclusions have been drawn from the dispersion curves. It was possible to identify which modes are more sensitive to cement defects, what reinforces the importance of simulation in the analysis. When comparing the slowness curves for the nominal and the cases with defective cement, modes G1 and G2 exhibit more significant changes for the through-tubing model, whereas, for the single-casing configuration, the mode R1 is more prominently changed.

In future works, we plan investigate other types of defects and other circumferential order modes, for instance by using monopole, dipole or quadrupole sources. As only subsonic modes have been studied, it is still important investigate supersonic modes, such as leaky modes, to find out if they are also sensitive to the presence of defects.

Acknowledgements

This research was funded by Repsol Sinopec Brasil under the ANP R&D levy as “Compromisso de Investimentos com Pesquisa e Desenvolvimento”. The authors also acknowledge the support provided by the Coordenação de Aperfeiçoamento de Pessoal de Nível Superior - Brasil (CAPES) - Finance Code 001.

Referências

ØIA, T. M., MATTS, M. A., & TORBJØRN, V. (2018). *Innovative Approaches for Full Subsea P&A Create New Opportunities and Cost Benefits*. SPE-191315: SPE Norway One Day Seminar. Society of Petroleum Engineers.

ØSTERBO, K. (2014). *Cement Bond Evaluation* (MSc Thesis). University of Stavanger.

BOERBOON, A. J, STAUFFER, D. B, & MCLAFFERTY, F. W. (1985). Ion Optics of Multipole Devices. I. Theory of the Dodecapole. *International Journal of Mass Spectrometry and Ion Processes*, *63*(1), 17–28.

BRAGA, A. M. B, BARBONE, P. E., & HERRMANN, G. (1990). Wave propagation in fluid-loaded laminated cylindrical shells. *Applied Mechanics Reviews*, *45*(5), S359–S365.

BRAGA, A. M. B., & RIVAS A., C. E. (2005). High-frequency response of isotropic-laminated cylindrical shells modeled by a layer-wise theory. *International Journal of Solids and Structures*, *42*(14), 4278–4294.

FAN, B., SKATARIC, M., BOSE, S., AERON, S., & ZEROUG, S. (2019). *Method of analyzing cement integrity in annuli of a multiple-cased well using machine learning*. US Patent Application: 62/577,945.

KHALIFEH M., & SAASEN A. (2020). Barrier Verification. In *Introduction to Permanent Plug and Abandonment of Wells* (Vol. 12). Ocean Engineering & Oceanography: Springer.

LIU, H. (2017). *Principles and Applications of Well Logging*. Springer Berlin Heidelberg: 237-269.

PLUTA, Mieczysław, & GRILL, Wolfgang. (2002). GRILL, Wolfgang. Phase sensitive acoustic microscopy image quality estimation by volume imaging in anisotropic media. In *Acoustical Imaging*. Springer: 213-221.

QUINTERO, L. F., ZHENG, Y., & KIRKWOOD, A. (2016). *CHARACTERIZATION OF WELLBORE MATERIALS IN MULTIPLE CASING STRINGS*. US Patent Application: 15/750,754.

SAXENA, V., KRIEF, M., & ADAM, L. (2018). *Handbook of Borehole Acoustics and Rock Physics for Reservoir Characterization*. Elsevier.

TALBERG, A. S., JOHANSEN, T. F., & LARSEN, I. (2017). *Laboratory Experiments on Ultrasonic Logging Through Casing for Barrier Integrity Validation*. ASME 2017 36th International Conference on Ocean, Offshore and Arctic Engineering: American Society of Mechanical Engineers Digital Collection.

VIGGEN, E. M., JOHANSEN, T. F., & MERCIU, I. (2016). Analysis of outer-casing echoes in simulations of ultrasonic pulse-echo through-tubing logging. *Geophysics*, *81*(6), D679–D685.

VIGGEN, E. M., JOHANSEN, T. F., & MERCIU, I. (2016). Simulation and modeling of ultrasonic pitch-catch through tubing logging. *Geophysics*, *139*(5), 2407–2416.

WANG, H., TAO, G., & SHANG, X. (2016). Understanding acoustic methods for cement bond logging. *The Journal of the Acoustical Society of America*, *139*(5), 2407–2416.

ZHANG, J., MAHBOD, P., SHAFER, R., MULLER, D., & ANDERSON, C. (2019). *Multi-String Isolation Logging - A Cost Effective Solution for P&A*. SPE-195607-MS: SPE Norway One Day Seminar. Society of Petroleum Engineers.